LEGIBILITY NOTICE

1

Received by ... TI

Nov 0 5 1989

TITLE A HYPERVELOCITY LAUNCHER FOR WELL PERFORATION

AUTHORS L. Erik Fugelso
James N. Albright
Gerald C. Langner
Kerry L. Burns

MASTER

Los Alamos
Los Alamos National Laboratory
Los Alamos, New Mexico 87545

A HYPERVELOCITY PROJECTILE LAUNCHER FOR WELL PERFORATION

L. Erik Fugelso. James N. Albright,
Gerald C. Langner. and Kerry L. Burns

University of California
Los Alamos National Laboratory
Los Alamos. NM 87545

ABSTRACT

Current oil well perforation techniques use low- to medium-velocity gun launchers for completing wells in soft rock. Shaped-charge jets are normally used in harder, more competent rock. A launcher for a hypervelocity projectile to be used in well perforation applications has been designed. This launcher will provide an alternative technique to be used when the conventional devices do not yield the maximum well perforation. It is an adaptation of the axial cavity in a high explosive (HE) annulus design, with the axial cavity being filled with a low density foam material. Two configurations were tested: both had an HE annulus filled with organic foam, one had a projectile. Comparison of the two shots was made. A time sequence of Image Intensifier Camera photographs and sequential, orthogonal flash x-ray radiographs provided information on the propagation of the foam fragments, the first shock wave disturbance, the projectile motion and deformation, and the direct shock wave transmission from the main HE charge. Perforation tests of both device configurations (with and without the pellet) into steel-jacketed sandstone cylinders were made. Static radiographs of the cavities in the sandstone showed similar cavities, however, the perforation of the steel cap was larger in response to the pellet. DYNA2D calculations were made to assist in the interpretation of the experimental records. The preliminary results show promise that a useful perforating tool can be developed. Plans for an extended experimental program are outlined.

INTRODUCTION

A study has been initiated at Los Alamos National Laboratory to evaluate the application of hypervelocity launchers for rock penetration from cased oil and gas wells. Current oil well perforation techniques use low- to medium-velocity gun launchers for completing wells in soft rock. Shaped-charge jets are normally used in harder, more competent rock. In this paper a device to create a much higher velocity projectile is proposed. This launcher will provide an alternative technique to be used when the conventional devices do not yield the maximum well performance. The overall goal of the study is to elucidate the effects of a hypervelocity penetrator on rock after passage through well casing, as contrasted with the well-known effects of the typical jet perforator, or shaped-charge perforator

As an initial step, a projectile driver was designed to accelerate a pellet to high velocity within the confining dimensions of typical oil and gas wells. In the basic design the projectile was driven by a jet produced by a foam-filled axial cavity contained in a tamped annulus of High Explosive (HE). Provision for lateral confinement, detonator leads and associated electronics, and end-on blast suppression were also included.

DYNA2D calculations of the detonation of the HE and the subsequent compression of the foam-filled cavity indicate that a high-velocity, compressed foam slug is developed. This foam slug, which resembles but is not exactly equal to a jet in the axial cavity, may be used either as the penetrator itself or as the driver for a small projectile. The mechanical properties of the foams were specified by the initial and fully compacted densities, the loading and unloading curves in the pressure-volumetric strain space, and the shear behavior, modeled as a von Mises elastic-perfectly plastic material. Design parameters that affect performance are details of the detonation of the annular explosive, the composition of the foam material, the ratio of the foam cavity diameter to the HE exterior diameter, the blast shield configuration, and device standoff and exit geometry.

A series of tests was designed to evaluate the basic design, to refine materials selection, and to study the performance of the launcher in penetrating rock. Two foam materials were selected and an axial cavity geometry was specified. In this preliminary phase of the program, two shots were fired. One organic foam and one projectile were selected: the experiments were conducted with and without the projectile to obtain preliminary information on the compressed foam plug and then on its effect on the projectile. Radiographs were taken of the foam mass as it exited the cavity, defining its shape and kinetic energy upon emergence. For each of these shots a witness plate was used to compare deformation from the projectile, and from the directly transmitted axial pulse from the compressed foam and HE. After this information is processed, shots will be fired into a sandstone target cemented in a confining steel jacket at standoff distances that are typical of the downhole configuration.

A discussion of the test results is included, which provides guidelines for the next iteration of device design, for refinements in target design, for post-test characterization, and for maximizing damage to the rock produced through fracturing. The preliminary tests show sufficient potential that further development is recommended.

BACKGROUND

Well Perforation Problem

Need for Penetrator/Perforator Petroleum fluids (oil and natural gas) are generated at a "source rock" by the decay of organic matter in an anaerobic environment. Because of their bouyancy, these hydrocarbons migrate along permeable beds in a generally upward direction until they are trapped by overlying or blocking geological structures (such as a low-permeability "cap rock") or by pinch-out effects. The region of the trap is the "reservoir rock" and contains both water and petroleum fluids.

The simplest way to provide fluid flow is to drill production holes into the reservoir and leave the bottom of the holes unlined. These are "open-hole completions". Oil drains into the well from the sides and is collected from the bottom of the hole.

Normally, to prevent sidewall cave-ins and overburden-induced pinchoff, the drillholes are lined with a steel casing, which is cemented in place. To provide for fluid access, holes are cut through the steel and cement into the reservoir rock. A perforating tool is used for this pupose. A series of radial holes are created which pass from the interior of the well, through the casing, and through the cement, into the surrounding rock. The results of the perforation are illustrated in Fig. 1. Hydrocarbons drain into these holes, flow along them to the wellbore, and are then pumped to the surface.

There are three methods of perforation. The first, gun perforating, which dates from 1932, uses a solid bullet, fired from a gun mounted inside the perforating tool, with the axis of the gun oriented transverse to the axis of the well (Sawdon, 1943). The second, jet perforating, which dates from 1948, uses a shaped charge with a liner. This fires a jet into the rock, (Birkhoff et al., 1948; Poulter Caldwell, 1957). The third is hydraulic

perforation, which is a high-pressure stream of particles (mainly water and drilling mud with an abrasive added), which abrades a hole in the rock (Thompson, 1963).

The gun should be matched to the size of the casing. There is an annular gap between the gun and the casing, the width of which is the "stand-off distance" between the gun and target. A small gun with a large stand-off distance in a large pipe has reduced penetration, because the projectile or shaped charge loses energy in penetrating the well fluid.

Space Limitations There are severe space limitations working inside a wellbore. The main limitation is the inside diameter of the well casing, typically of the order of 10 to 20 cm. A second constraint is the transverse dimension of the perforating string.

Typical Perforation/Penetration Data

The depths of perforation in typical reservoir rocks ranged from 7 to 30 cm for bullets and 10 to 45 cm for shaped charges (McConnell, 1957). Thompson (1963) examined the effect of compressive strength upon penetration. For both bullets and shaped charges, the diameter of the perforation hole decreased as compressive strength increased. Penetration is best with bullets in soft formations, and with shaped charges in medium to hard formations. Thompson's results imply a similarity between the processes of jet and hydraulic perforating. Depth of penetration is controlled more by gun diameter than by charge weight (Bell and Shore 1965).

The shape, depth, and other details of perforations cannot be determined in the field. A standard test procedure has been designed by the American Petroleum Institute (Krueger, 1985). The information on perforations comes from laboratory tests made according to that standard (e.g. Bell and Shore, 1956; Halleck and Deo, 1989).

Under some test conditions, the rock fractures extensively, while in other tests, it does not. With properly prepared specimens, damage to the rock caused by shaped charges consists of a "halo" of compaction and pulverization products (Krueger, 1956), due to plastic yield around the perforation (Birkhoff et al., 1948; Allen and Worzel, 1956; Halleck and Deo, 1989). Bullets do not seem to crush the rock to the same extent, and there are reports of cracking ahead of the bullet.

The usual shape of bullet holes is cylindrical, with a diameter equal to that of the bullet. Perforation holes due to shaped charges have the shape of a tapered cylinder or cone. (see Fig. 2).

In practice, shaped-charge perforations are not clean, fresh exposures of wall rock. In some cases a plug obstructs the hole in the steel liner. In other cases a carrot may plug the hole in the rock, composed of the material derived from the shaped-charge liner, or debris fallen back from the damage halo (Allen and Worzel, 1956). In other cases, the crushed and compacted debris in the damage halo, or compacted mud swept out of the drilling fluid, may form an impermeable film on the rock and plug the formation.

Neither bullet nor jet perforation yields consistent and predictable results for the creation of a flowing well. For those wells that need only an opening between the drillhole and the rock matrix, the mechanism is known and reliable. For those wells wherein the perforation process must open fluid flow channels, the mechanism is less well understood.

EXPERIMENTAL PROBLEM

Experimental Background

Woodhead (1947 and 1959) demonstrated that, in a tubular charge of high explosive with air as the material that filled the axial cavity, a very high pressure shock wave could be generated in the air cavity. Woodhead and Titman (1965) reported a series of experiments on cylindrical annuli with the axial cavity filled with air. They showed that the mean detonation velocity in the cylinder was slightly higher than in a solid piece of HE and that a shock wave had been formed in the axial cavity. In a tubular piece of HE with an air-filled axial cavity, the shock wave generated in the cavity had a steady velocity about 1.75 times that of the detonation wave in the HE. Further, the detonation wave in the HE was enhanced by about 5% due to the symbiotic effect of the the pressure wave generated by the air shock. The pressure in the axial cavity shock wave was significantly stronger than the shock wave directly transmitted to the air from the plane end of the annular HE and had considerable force. This was demonstrated by the crater generated in a witness plate. The craters generated from the HE with the cavity were a deep, narrow cavity, which was formed first from the cavity air shock, and a broader, shallower crater from the main blast. This second crater was essentially the same as the one created by the blast from a solid cylinder of HE. Ahrens (1965) made measurements on the blast, cratering, and perforation induced by a 70-mm-long, 50-mm-diameter cylinder with a variety of axial cavities. This tubular HE was ignited by the single-point detonation of the solid cylinder of HE with the same exterior dimensions. The diameters of the axial cavities ranged from 1 mm to 40 mm. This device created a jet or central slug of air that perforated a 40 mm thick plate of armor steel. No perforation was noticed with either pure HE or with an annulus with a very large axial cavity. The optimum perforation was obtained with a cavity diameter of 6 mm. Cratering and spalling were noted in all cases.

Koski et al. (1952) conducted a series of experiments on cylindrical annuli of HE with very thin metallic liners and with a vacuum within the liner. Their initiation mechanism was the same as the one in our present device. Rather than using the effective plane-wave generation in the annular segment of the HE as in the cases above, they created an effective outer-rim-circle source by using first a single-point detonator that ignited a cylinder of HE, which was attached to the HE tube. A smaller diameter brass disk, backed by a foam disk at the base of the HE cylinder, prevented immediate propagation of the detonation wave. The detonation wave was thus forced to communicate with the HE annulus at the outside of the brass plate. They reported jet or slug velocities emerging from the axial cavity in excess of 70 km/s. The jet material was from the very thin liner and there wasn't much of it.

Wenzel (1987) reviewed other explosively driven projectile launchers with similar configurations. In particular, he reported that cylindrical pieces of HE with axial cavities filled with air had been used as projectile drivers in the early 1960s. He also reviewed an unpublished report by Garza in 1982, which stated that the projectile driven by the air shock in such a device was extremely deformed during the launch.

Further development of related devices continues. Three current examples are cited. McCall (1984) described a device for hypervelocity projectiles using an annular piece of HE, which was lined with steel and partially filled with foam. The remainder of the cavity between the foam and a small projectile placed at the opposite end of the liner was under a vacuum. The HE was detonated at one end and an one-dimensional shock wave was induced in the foam segment. The foam expanding into the vacuum eventually struck the projectile and a very gentle acceleration of the projectile ensued. McCall (1984) attributed the genesis of this concept to Stirling Colgate. The detonation of an annulus of HE surrounding a rod of polyethylene was modeled and tested by Adams et. al. (1987). The calculation was divided into component parts: the formation of the rim initiator, the main phase during which the detonation wave propagates along the HE annulus and strongly compresses the foam rod, and the subsequent interaction of this wave with an

expansion nozzle and a gun barrel. Marsh, et al. (1989) reported a similar hypervelocity launcher. They used a 76.2 mm (3 in.) diameter by 76.2 mm (3 in.) long cylinder of PBX 9501 to drive a 19.1 mm (0.75 in.) diameter, 0.8 mm (1/32 in.) thick pellet of 304 stainless steel to a velocity of 6.4 km/s. The HE was detonated at a single point on its rear face. The projectile was fired down a two-stage barrel, with 50.8 mm OD for the first 50 mm length and 25.4 mm OD for the remaining 100 mm length. Their projectile has a 1.6 mm (1/16 in.) standoff from the 9501 cylinder.

Description of the device

The HE launchers described in the previous section utilized either a very low pressure gas in the axial cavity, in which case the shock wave in the cavity attained an extremely high velocity; air at atmospheric conditions, in which case the shock in the cavity was slightly higher than the detonation velocity; or a very light density organic foam. In this latter case, very high velocities were predicted along the axis, possibly due to phase changes in the compressed foam (Adams, et al., 1987).

Figure 3 shows the drawing of the experimental device. The main component is the cylindrical annulus of PBX 9501 HE. The axial cavity has a diameter of 6 mm, which was the optimum diameter in Ahrens' work. The device is initiated at a single-point slapper detonator, with a PETN booster located on axis at the rear of the specimen, which detonates a 3.2-mm disk of PBX 9407. The rim initiation in the HE annulus is provided by the insertion of a foam-backed brass disk between the PBX 9407 disk and the PBX 9501 annulus. The axial cavity may be filled with air at atmospheric conditions or filled with a foam cylinder. The radial exterior of the HE is encased in a 3-mm thick brass cylinder. At the front base of the HE is a 6.35-mm (0.25 in) thick steel blast suppression plate. This plate has a 6-mm minimum diameter hole, which is tapered at 20° to permit passage of the either the cavity air shock or the compressed foam slug. A small steel pellet, 6-mm diameter and approximately 1-to 3-mm thick, may abut the foam cylinder.

Finite Element Calculations

The finite element code, DYNA2D, (Hallquist 1984) was used to perform preliminary evaluations of the development and evolution of the compressed foam slug. The portions of the device modeled are the high explosive annulus, the foam filler that lies in the axial cavity, and the exterior cartridge case. The brass modeled in this simulation was a 70% Cu - 30% Zn alloy, designated Cu 26000, and commonly known as cartridge brass. The HE is PBX 9501 and is described by a Jones-Wilkins-Lee (JWL) equation of state. The ignition of the HE in the device is simulated by detonating the HE over a washer-shaped area at one plane end of the annulus. The boundary condition at the opposite end of the HE, which simulates the blast suppressor plate, is approximated as if it were a rigid wall.

The constitutive equation for the foam is described in the manual for DYNA2D (Hallquist 1984). The foam is described by two curves, the pressure-volume curve in initial loading, unloading, and reloading, and a shear stress-shear strain curve. A typical pressure-volume curve is shown in Fig. 4. The octahedral shear stress-octahedral strain curve is a Drucker-Prager curve with no work-hardening and a yield stress dependent on the pressure. The measured properties of the foams of interest are very scarce. Limited data on the pressure-volume curves in loading, unloading, and reloading were available, so approximate curves were generated. Taylor (1975, summarized in Mader (1980)) measured the Hugoniot properties of foamed polystyrene. The initial density was 0.25 g/cm^3, the final compacted density approximately 1.1 g/cm^3 and the maximum value of the unloading bulk modulus from a peak pressure of one Mbar was about 10 times that of the initial elastic loading bulk modulus. The pressure-volume constitutive equation used in the calculations was approximated as piecewise linear. The value of the unloading bulk modulus was varied between the initial elastic modulus, which was approximated as

100 kbar. and ten times that value. Several runs were made for each foam material to bound the behavior of the compressed foam rod.

The qualitative behavior of all the computer simulations is described by the following steps. The detonation is initiated at the outside rim of one end of the HE annulus. A detonation wave propagates from that point, striking the foam rod and compressing it. As the detonation proceeds along the rod-HE interface, the rod is compressed. The phase velocity is infinite initially, then decelerates. A convergent shock wave propagates into the foam rod. compressing the foam to the density of the main constituent material. Behind this first shock, a faster rarefaction wave overtakes this initial shock. The radially convergent shock reflects (actually, interacts with itself) from the symmetry axis and propagates outwards, again with an overtaking rarefaction in pursuit. A Mach stem is eventually formed on the axis, which is manifested in a central slug of compressed foam moving along the axis with an appreciable velocity. Figure 5 shows the contours for axial

stress for planewave initiation in the HE annulus at 3.0 μs after initiation. Figure 6 shows the peak axial velocity as a function of position along the axis for two typical foams. One foam is described by an initial density of 0.4 g/cm^3, an unload-reload bulk modulus of 100 kbar, an initial compaction strength of 1 kbar, and a compacted density of 1.0 g/cm^3. The second foam is the same except for the unload-reload bulk modulus. which is 1 Mbar.

The comparison between plane initiation and rim initiation on the evolution of the peak particle velocity is shown in Fig. 7. Several different foam models were evaluated. The qualitative shape of the evolution of the peak foam velocity as the detonation sweeps along the length of the rod remains the same: a rapid initial growth, followed by a slower rise to a mature state (which would approach a steady state if the rod were long enough) and terminated by the reflected shock from the blast plate. Depending on the initiation model, the maturing phase may be either a slow rise to or a slow decrease from a maximum. This latter-case prediction occurs when the unloading bulk modulus is very stiff. The peak foam slug velocity that is attained at the end of the rod approaches 5 to 6 km/s for the various approximations used. This development of a small slug; which initially forms just behind the shock front, extends its size, and then matures into a slowly growing quasi-projectile; bears a qualitative resemblance to the formation of the luminescent shock in the axial cavity in the experiments by Ahrens (1965) and Woodhead and Titman (1965). Estimates of the kinetic energy in the foam slug; obtained using this velocity. the maximum compressed density of the foam, and the dimensions of the slug (from the finite element calculation) which are 0.5-cm thick and 0.3-cm radius: are approximately 1 to 2 kJ.

The high velocity compressed foam slug may be used to perforate the well casing and rock matrix directly or may be used to accelerate a small projectile that would be placed in the orifice at the end of the cavity. Because of the space constraints on the total device. the acceleration of the projectile is likely to be inefficient. First, the foam slug has an extreme radial gradient and. thus. the pressure applied to the projectile is not uniform. Second. the momentum transfer from the foam slug to the projectile involves the transmission of a high intensity. non-uniform shock wave. and the introduction of a nonuniform rarefaction to the blast plate cover and the high pressure burnt gas. The structure of the pressure pulse on the projectile will be diminished rapidly from its theoretical maximum. Since the projectile has the shape of a very thin disk (to minimize the transfer time of the momentum from the foam slug to the projectile and to maximize the projectile energy and momentum in the short interval permitted), the projectile will undergo severe distortion. Fedderson et al. (1968) showed that a thin plate of material will distort. stretch. and thin drastically in response to a dynamic pressure pulse and various edge constraints.

TEST RESULTS

Tests on two configurations are reported in detail in this paper. The axial cavity in both was filled with a low density foam and both had the blast suppression plate. One of these configurations was also fired with a small steel projectile. The purposes of these shots were to determine the properties of the foam slug and thence to ascertain the motion of the steel projectile that might be accelerated by the foam plug. Then perforation tests into a steel-jacketed sandstone specimen were to determine the cavity formation in a typical field configuration. For each configuration a diagnostic shot with x-rays and a perforation test were made. The foam used in these tests was polyurethane with an initial density of 0.35 g/cm^3.

In this series of tests, two orthogonal flash x-rays were taken to determine the position of the foam slug and the projectile as they exited the blast suppression plate. The x-rays were 150 keV. A sequence of four Image Intensifier Camera (I^{2}C) images were taken at selected times after initiation. The light source was an explosively driven argon candle. Figure 8 shows the typical layout of the experimental test. The locations of the specimen, the x-ray heads, the film cassettes, the argon light source, and the I^{2}C device are shown. Additional blast shielding to protect the x-ray head and the film cassettes is not shown.

Both of the configuations were fired into steel-jacketed sandstone cylinders. The sandstone cylinders were 15.24 cm (6.0 in.) long, 15.24 cm (6.0 in.) in diameter. The steel jacket was made from 1018 mild steel and was 0.635 cm (0.25 in.) thick. Epoxy was used to fill the gaps between the sandstone specimen and the jacket. However, these specimen tests do not match up to the API (Krueger 1985) test program criteria for well-perforation simulation. To meet these concerns, an additional fluid immersion system will need to be designed.

Preliminary Test

A preliminary test was performed with only the confined annulus of high explosive and the blast suppression plate to confirm the Woodhead and Titman (1965) and Ahrens (1965) test results for this size device. No pellet was used and the axial cavity was filled with air only. The device was placed in contact with eight 1/4 in. (0.635 cm) thick plates of 1018 steel with the axis of the annulus normal to the interface. When the device was detonated, a perforation cavity was formed with a depth of 15 mm (0.60 in.). The perforation is shown in Fig. 9.

Test Configuration 1 - Axial Cavity Filled with Foam, No Projectile

The main annulus of PBX 9501 was 36.7 g., the PBX 9407 booster pellet was 2.7 g, and the PETN booster was 0.8 g. The orthogonal flash x-rays were taken at 32.59 μs and 39.49 μs after the initiation of the detonation sequence, respectively. Figure 10 shows the later flash x-ray image. The foam that filled the cavity has broken up into a sequence of cubically shaped small particles with a typical size of 1 mm. The maximum velocity of the fragments is 5.5 km/s and the average velocity in the field of view is about 4 km/s, which agrees with the range of particle velocities in an HE cylinder with an air-filled cavity as reviewed by Wenzel (1987). If the foam particles have been compressed to maximum density, the lead particle has about 20 kJ of kinetic energy.

Figure 11 shows the first of four I^{2}C images, taken at 20 μs after initiation. The propagation of the leading edge of th : air shock is 7.8 km/s. The expansion gas cloud, pictured on the I^{2}C images, completely contains the group of discrete particles shown on the radiograph. The edge of the blast suppression plate has a velocity of 3.2 km/s, which, if interpreted as twice the particle velocity in the incident shock, implies a reflected pressure in the HE annulus of about 750 to 800 kbar (which is consistent with the

estimated reflected shock pressure in the annulus or approximately twice the detonation pressure). The first witness plate, 0.953 cm (0.375 in.) 1018 AISI steel was 25 cm from the base of the blast suppression plate. Three hemispherical craters approximately 0.3 - 0.6 cm (0.125 - 0.25 in.) deep were noted, which is consistent with impact by the observed fragments.

The perforation test into the steel-capped sandstone cylinder yielded a cavity 27 mm deep and a perforation hole in the steel about 5 mm in diameter. The blast suppression plate of the device was positioned atop the steel-sandstone cylinder with a stand-off distance of 0.47 cm (3/16 in.).

Test Configuration 2 - Axial Cavity Filled with Foam, Steel Projectile

The configuration for this test was the same as for the previous test except that a small stainless steel (SS304) cylindrical disk, 6 mm diameter and 2 mm thick was glued on the end of the foam cylinder. Figure 12 shows a typical flash radiograph at 40.87 μs after initiation. The steel projectile is emerging from the blast plate orifice. Results for the motion of the gas cloud, small foam fragments, and blast suppression plate were obtained in this shot and were almost identical to those of the previous configuration. The gas cloud and the foam fragments appeared to be a part of the blow-by that preceded the pellet. The pellet had a normal velocity of 1.5 km/s as it passed the blast suppression plate. A small number of significant craters were observed in the witness plate. No specific crater could be identified as being generated by the projectile. Asssuming that a constant pressure was acting on the pellet during the time it was exiting the suppression plate, that pressure is estimated at approximately 14.5 kbar. This compares with the mean pressure of 16 kbars implied in the Marsh et al. (1989) experiment.

The perforation test into the steel-capped sandstone cylinder yielded a cavity 25 mm deep and a perforation hole in the steel about 8 mm in diameter.

Comparison of the Two Test Configurations

The main disturbance from both test configurations is the gas blowby. Embedded in this rapidly expanding cloud are many high-velocity foam fragments. The distribution and velocities of these feaures are essentially the same for both devices. Motion of the blast suppression plate indicates that the detonation was the same in both configurations and was that expected. The pellet, present in only one test configuration, had a fairly low velocity. This is to be expected since the pellet had only a short run under pressure which, however, matched the internal pressure of a much higher velocity gun. Figure 13 shows the static post-shot radiographs of the cavities in the steel-capped sandstone cylinders. Figure 14 shows the perforation holes in the 1018 steel cap for the two configurations. The perforation width with the pellet is wider, but the depth of the crater is about 2 mm less. These specimens will be sectioned. The number and extent of the newly formed microcracks will be measured and reported elsewhere.

CONCLUSIONS AND FUTURE PLANS

The design and preliminary testing of a hypervelocity launcher for the oil well perforation process have been completed. The device, which must meet severe size and explosive charge restrictions, is an adaptation and amalgamation of three old configurations, the concepts for which date back at least forty years. The basic device is a tamped cylinder of HE with a small diameter axial cavity. The cavity is filled with a low density foam, either organic or metallic. The HE annulus is detonated at the outside rim by means of a wave shaper. The material in the axial cavity is rapidly accelerated by the action of the convergent detonation and shock waves. A highly compressed (and possibly ionized)

slug of foam is propelled down the axial cavity. A mixture of burnt detonation gases and the foam is ejected from the HE. A blast suppression plate at the end of the HE has a small orifice to permit passage of the compressed material in the axial cavity while reflecting and retarding the pressures in the main detonation wave.

Tests on two configurations were reported here. The first test configuration has only a foam-filled axial cavity, while the latter adds a small steel projectile which is initially at the end of the axial cavity. In the first test the foam cylinder was accelerated to fairly high velocities and broke up very quickly into small fragments. The fragment velocities ranged from about 2 to 5.5 km/s and several of the fragments were approximately 1 mm^3. The leading edge of the disturbance as shown by the I^{2}C images had a velocity of about 7.8 km/s. The blast that propagated through the blast suppressor plate arrived significantly later than the other two phenomena. The pellet was accelerated to the fairly low velocity of 1.5 km/s in the very short launch distance. The effective pressure acing on the pellet was about the same as that generated by Marsh et al. (1989). The burnt gases and the foam fragments blew by the projectile and have about the same velocities and energies of the test without the pellet. The motion of the blast suppressor plate was the same in both tests.The foam plug and projectile acceleration for one foam and one HE configuration are thus determined.

Perforation and penetration tests of the two device configurations into a steel-jacketed sandstone cylinder were carried out. The penetration depth into the sandstone was similar, with the penetration from the device with no pellet being slightly deeper. Perforation of the steel cap was greater with the steel pellet. We hus conclude that the major contributions to the force acting upon the sample come from the expanding burnt gases and the fragmented foam cylinder. The contribution from the pellet is limited.

The preliminary test results shown in this paper indicate that a high velocity projectile and a stream of small, high velocity compressed foam particles can be generated in a small, confined volume. Either configuration perforates the steel plate modeling the casing and generates a significant cavity in the sandstone cylinder. This design thus adds another tool for downhole perforation. To continue exploration into the utility of this device in its intended application, a more extensive series of experiments has been planned in the continuing phase of this program. A second, denser, organic foam will be examined as will two densities of copper foam. Again, selected combinations of foam alone and foam with a small projectile will be examined.

Since the main purpose of this program is the development of a high velocity gun for oil well perforation, several experiments wherein either a high velocity foam plug or the pellet will be driven into steel-jacketed sandstone cylinders have been carried out to determine the perforation parameters. Perforation creates consistent and predictable results for accessing the fluid in the rock formation in a completed well. For those wells that need only an opening between the drillhole and the rock matrix, the mechanism is known and reliable. For those wells wherein the perforation process must open fluid flow channels, the mechanism is less well understood. Techniques to determine the number, extent, and quality (inter- or intra-granular) of the fractures induced (created or extended) by the impact and the changes in porosity, are under current development and will be reported elsewhere.

ACKNOWLEDGMENTS

REFERENCES

Adams. T. F., S. T. Bennion, W. B. Harvey, and T. H. Tan (1987). The fast shock tube - hydro calculations and experiments, Los Alamos National Laboratory Internal Report (unpublished report).

Ahrens, H (1965). Über den Detonationsvorgang bei Zylinderischen Sprengstoffenladungen mit axialer Höhung, Explosivstoffe, 13, 124-134.

Allen, T. O. and H. C. Worzel (1956). Productivity method of evaluating gun perforating, Drilling and Production Practice, American Petroleum Institute, New York. 112-125.

Bell, W. T. and J. B. Shore (June,1965). Lab studies show why and how gun perforators damage casing, The Oil and Gas Journal, 1009-1018.

Birkhoff. G., D. P. MacDougall, E. M. Pugh and G. I. Taylor (1948). Explosives with lined cavities, Jour. Applied Physics, 19, 563-592.

Fedderson. D. W., L. E. Fugelso F. E. Ostrem and E. B. Watts (1968). Investigation of gas detonation forming on aerospace materials, AFML-TR-68-3, Air Force Materials Laboratory (unpublished report).

Halleck, P. M. and M. Deo (1969). Effects of underbalance on perforation flow, SPE Production Engineering, 113-1116.

Hallquist, J. O. (1980). User's manual for DYNA2D -- an explicit two-dimensional hydrodynamic finite element code with interactive rezoning, University of California, Lawrence Livermore National Laboratory, Report No.UCID-18756 (unpublished report).

Harris. M. H. (Dec., 1956). A closer look at perforating, Petroleum Engineer.

Koski, W. S., F. A. Lucy, R. G. Shreffler and F. J. Willig (1952). Fast jets from collapsing cylinders, Jour. of Applied Physics, 23, 1300-1305.

Krueger, R. F. (1956). Joint bullet and jet perforation tests, in Drilling and Production Practice, American Petroleum Institute, New York, 126-140.

Krueger, R. F., ed. (1985). API recommended practice, standard procedure for evaluation of well perforators, American Petroleum Institute,Washington, D. C., 4th edition, 18 pp.

Mader, C. L. (1980). PHERMEX Test Results, vol. 3, 396-399, University of California Press, Berkeley, CA.

Marsh, S. P., R. G. McQueen and T. H. Tan (1989). Acceleration of metal plates, Shock Compression in Condensed Matter - 1989, AIP Topical Conference, ed. J. N. Johnson, (to be published).

McCall, G. H. (1984). A method for producing shockless acceleration of masses to hypervelocities using high explosives. La Jolla Institute Report. LJI-TM-84-106, (unpublished report).

McConnell, L. V. (Dec., 1957). Pros and cons of jet and bullet perforators, World Oil, 169-170.

Poulter, T. C. and B. M. Caldwell (1957). The development of shaped charges for oil well completion. Petroleum Transactions AIME, 210, 11-18.

Sawdon, W. A. (Oct., 1943). New bullet design for gun perforating, The Petroleum Engineer, 206-207

Thompson, G. D., (1962). Effects of formation compressive strength on perforator performance, in Drilling and Production Practice 1962, American Petroleum Institute, New York.

Wenzel, A. B. (1987). A review of explosive accelerators for hypervelocity impact, Intern.Jour. of ImpacEngineenng, 5, 681-692.

Woodhead, D.W. (1947). Velocity of detonation of a tubular charge of explosive, Nature, 160, 644.

Woodhead, D.W. (1959). Advance detonation in a tubular charge of explosive, Nature, 183, 1756-1757.

Woodhead, D.W. and H. Titman (1965). Detonation pl. nomena in a tubular charge of explosive, Explosivstoffe, 13, 113-123.
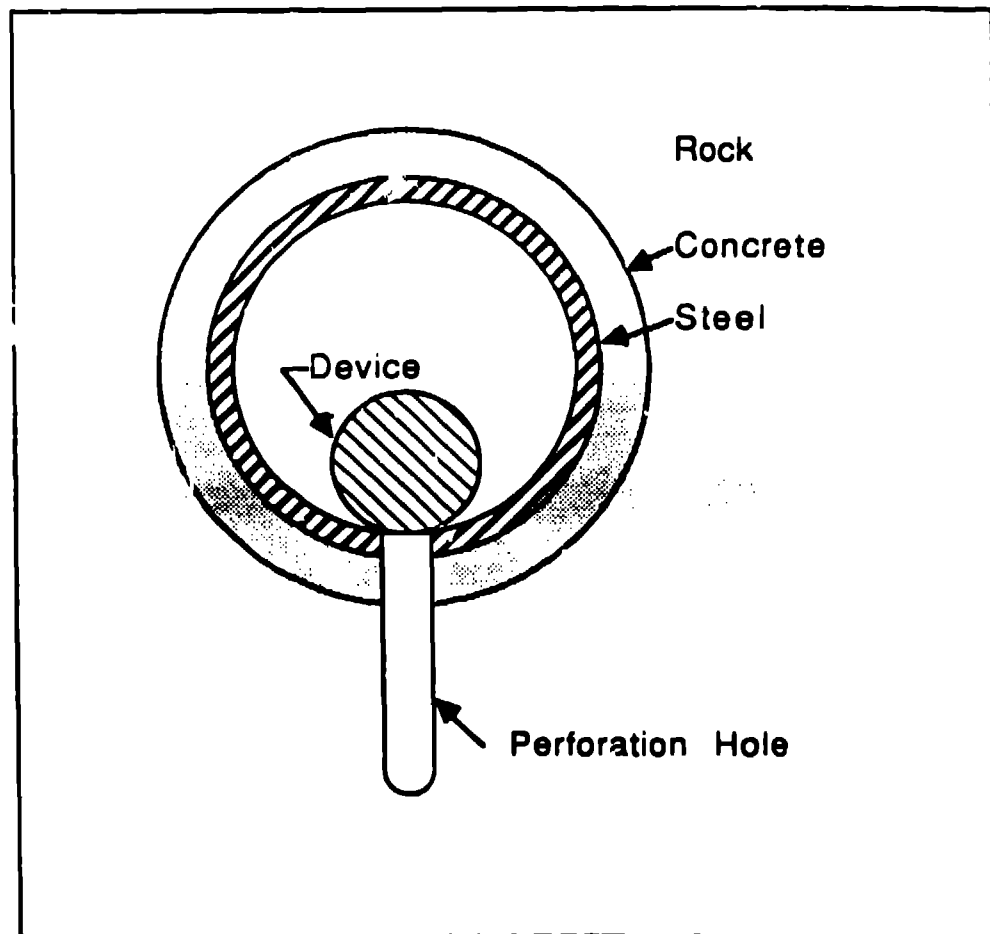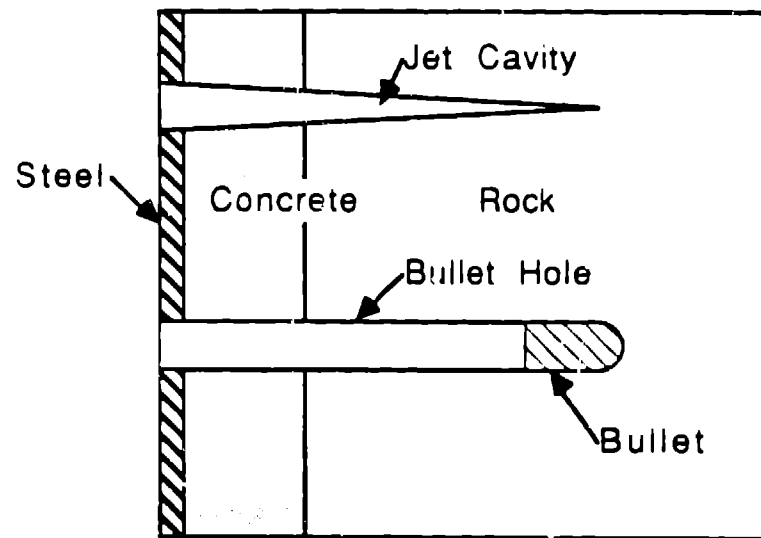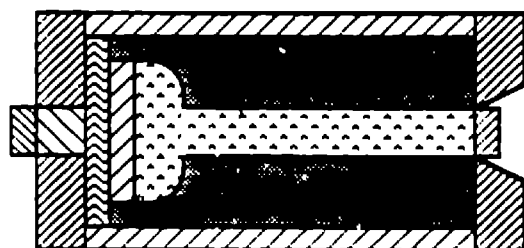
Fig. 1. Schematic of well perforation device

Fig. 2. Jet and bullet perforation

Scale 1 cm

▨	STEEL	■	PBX 9501
▨	BRASS	▨	PBX 9407
▨	FOAM	▨	SLAPPER DETONATOR
▨	PETN		

Fig. 3.   Schematic of the device
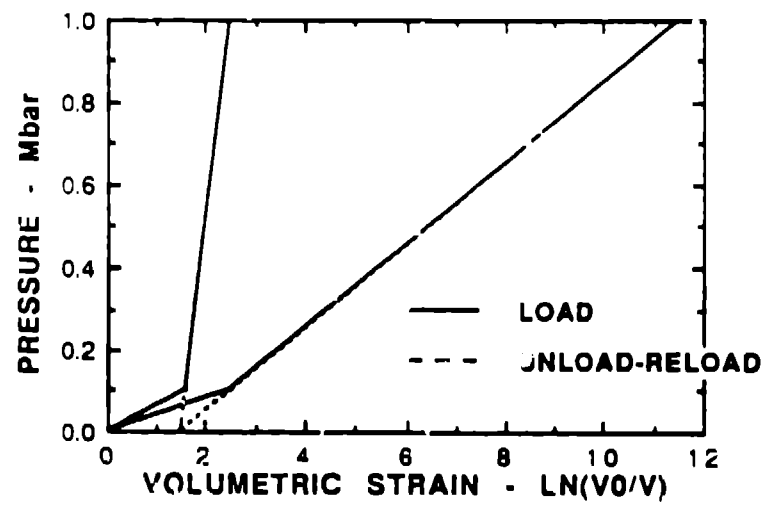
Fig. 4.   Pressure versus volumetric strain for the foam

Axis of
Symmetry

BURNT HE

STRESS CONTOURS
GPa

A	-38.0
B	-32.9
C	-27.9
D	-22.9
E	-17.8
F	-12.8
G	-7.76
H	-2.72
I	+2.31

FOAM

BRASS

UNBURNT HE
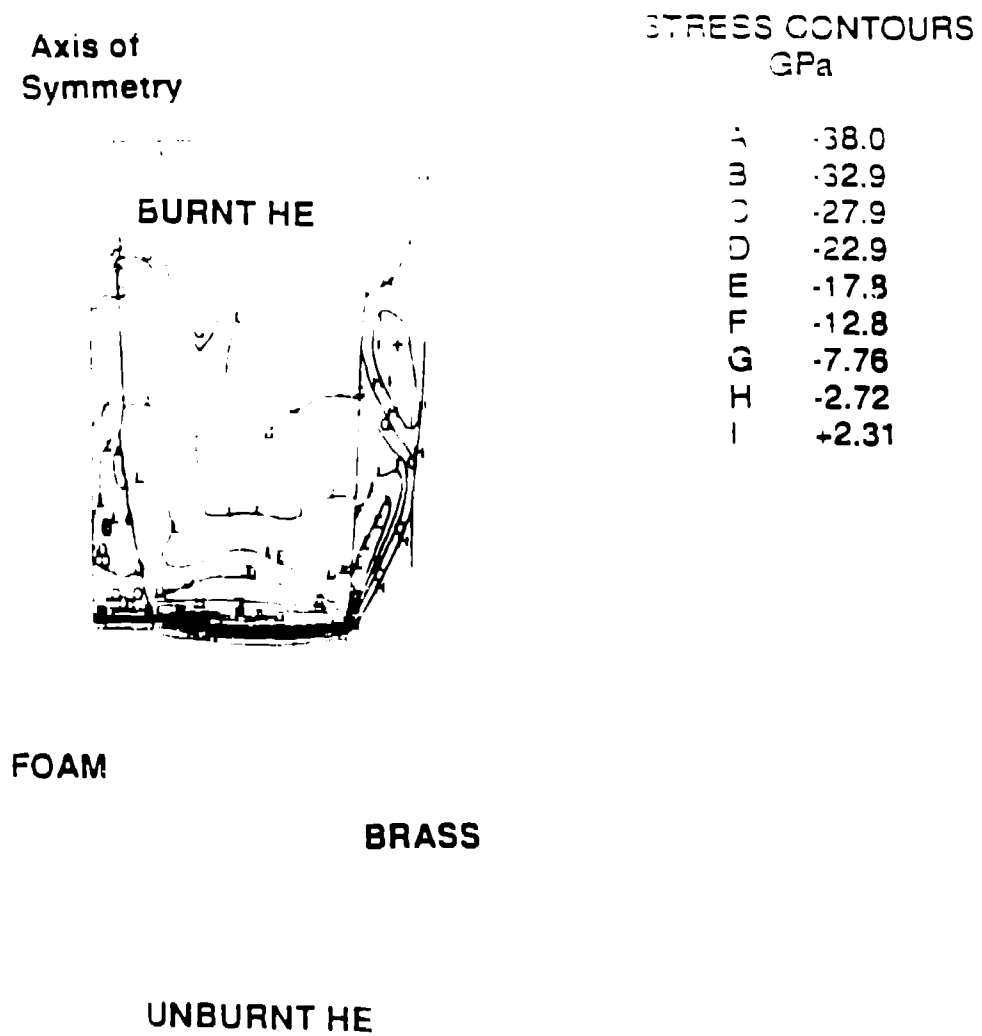
Fig. 5. Contours of axial stress at 3 μs plane-wave initiated
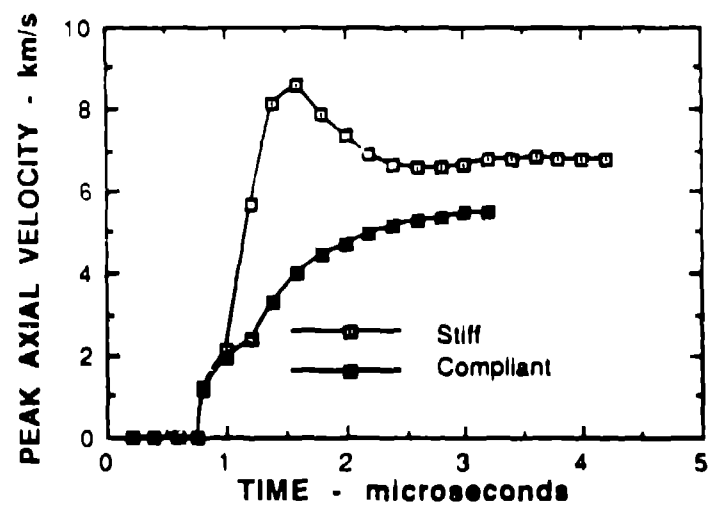
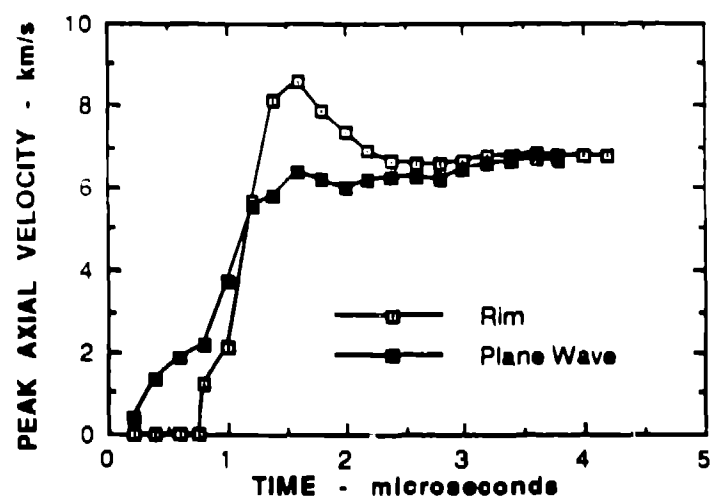Fig. 6. Comparison of foam models - peak axial velocity in the foam versus time

Fig. 7.   Rim-fired versus plane-wave initiation models -
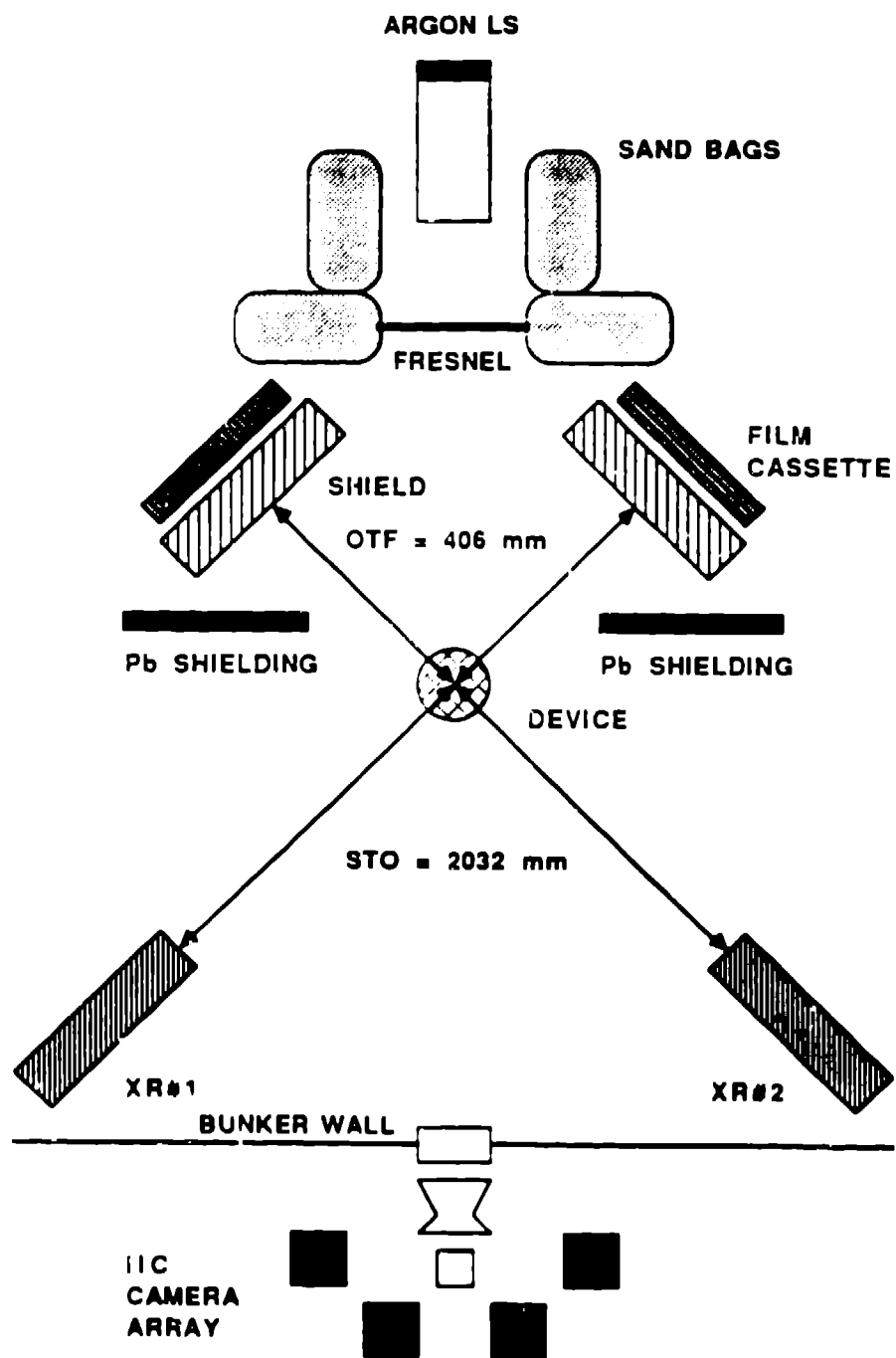peak axial velocity in the foam versus time

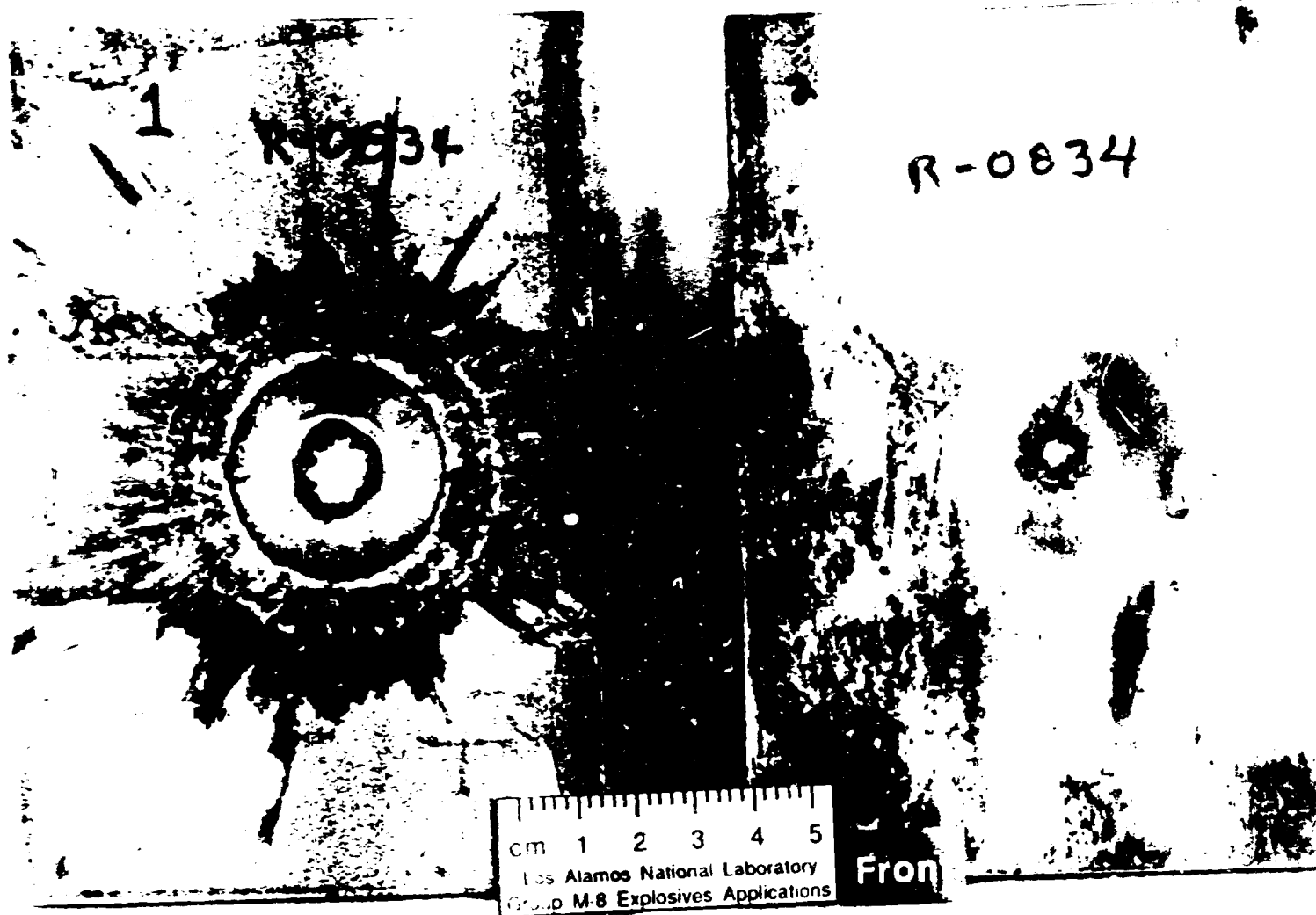Fig. 8.   Typical layout for the experimental test

Fig. 9.   Preliminary plate perforation test of the device without pellet and foam plug

Figure ... The ... ... with in the pellet ... ...

Fig. 11. PIC image of the shot without the pellet at 20.00 µs

Fig. 12. PIC image of the shot with the pellet at 40 µs

Fig. 13. Comparsion of the post-shot X-rays of the perforation craters in the jacketed sandstone specimens

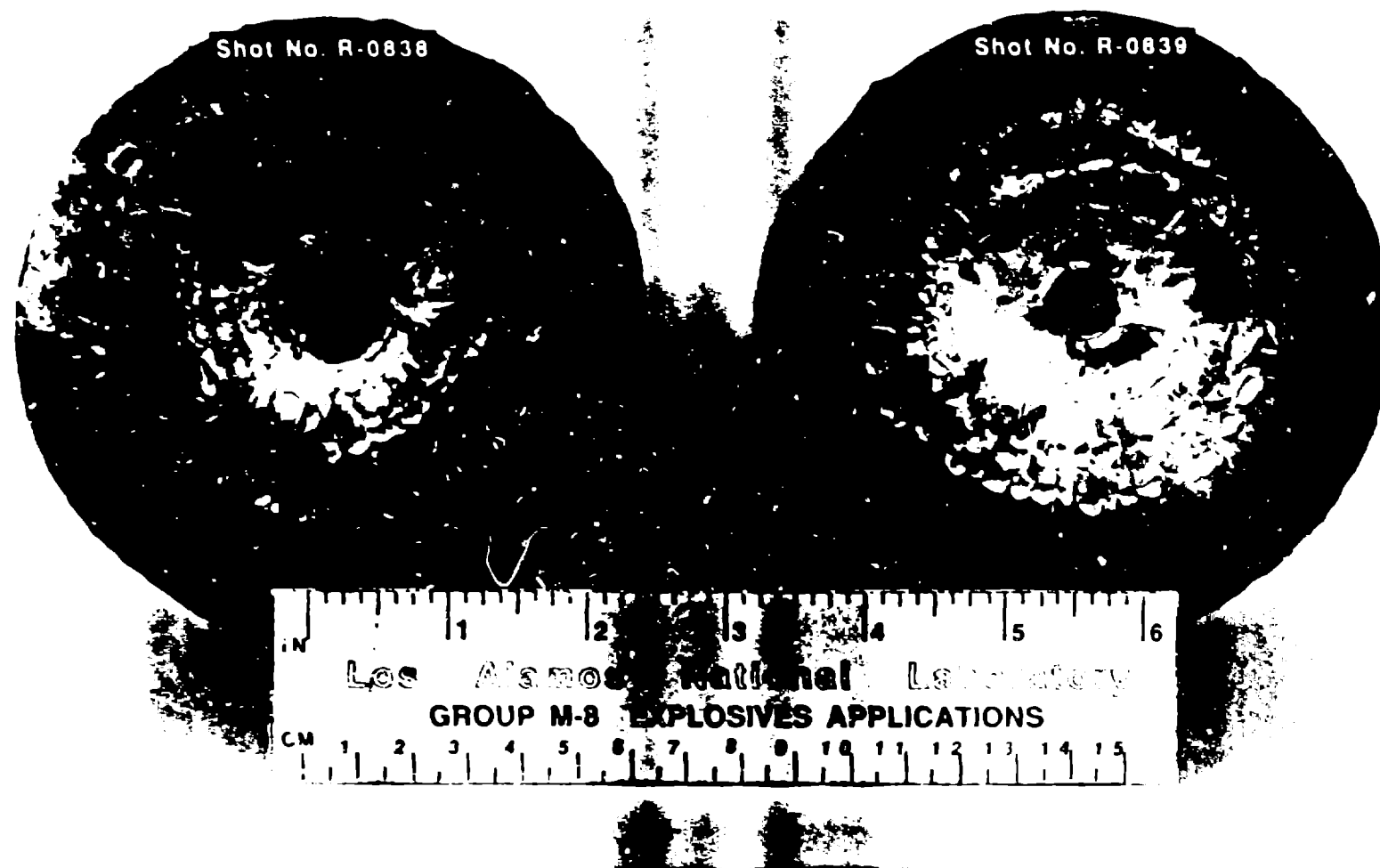Left - with projectile. Right - without projectile

Fig. 14.   Comparison of the perforation holes in the jacketed sandstone specimens
Left - with projectile. Right - without projectile